Valeology: International Journal of Medical Anthropology and Bioethics (ISSN 2995-4924) VOLUME 03 ISSUE 3, 2025

INVESTIGATING THE IMPACT OF SINGLE SLOTTED FLAPS ON WING AERODYNAMICS: A CFD STUDY ON THE CESSNA C208B

Mhmood H. Hami, Nadhim M. Faleh

Mechanical Engineering, Mustansiriyah University, Baghdad-Iraq

Abstract:

Two interacting boundary layers create a three-dimensional separation when fluid flows through a wing. The performance of the airfoil may be negatively impacted by the secondary flow that results from this separation. Up until now, airplanes have frequently used slotted flaps that can avoid separation and lower the resistance value. The current work presents an experimental and numerical investigation into the performance and aerodynamics characteristics of a new single-slotted flap mounted on a Cessna 208b Grand Caravan wing. Numerical simulation using the ANSYS-Commercial CFD package is the approach used herein. A revised Cessna 208b wing with a Grand Caravan single-slotted flap in three flap angles of $\alpha F = 0^{\circ}$, 15°, and 30° that researches the performance on its aerodynamics. Ranging from angles of attack $\alpha = 0^{\circ}$, 8°, 14°, 16°, and 18°. The fluid used is air, and under conditions of stability, has a cruise speed of 96 m/s at sea level altitude. Observe that a Cessna C208b Grand Caravan aircraft performance and wing's aerodynamic properties will be changed, which has been obtained in the addition of flap angle through simulation. As seen, it can be clearly told that at higher angles of attack with flow separation, because of intensification of turbulence, a higher flap angle may lower the value to 10.20 at $\alpha F = 30^{\circ}$ and $\alpha = 8^{\circ}$ at 96 m/s. However, at low angles of attack, the addition of the flap angle at $\alpha F = 0^{\circ}$ and $\alpha = 8^{\circ}$ may yield a higher value of CL/CD, amounting to 13.80, which is an indication of better aerodynamic efficiency. The vorticity patterns observed also indicate larger and more dispersed vortices at higher flap angles, contributing to drag buildup and reduced efficiency.

Keywords: CFD (Computational Fluid Dynamics), Pressure Coefficient (Cp), Lift to Drag Ratio (CL/CD), single slotted flap, Aerodynamic Performance.

1. INTRODUCTION

In flow over a wing, two interacting boundary layers will cause separation three-dimensional. Separation thus caused will be responsible for secondary flow which reduces performance of airfoil. A consequence of such loss will be the reduced effective area that may be able to generate lift [1]. The flap is the most generally used high-lift device in aircraft. The flap enables a compromise to be made among reasonably low landing speed and high cruise speed, since it may be retreated inside the wing framework when not utilized and extended once lift is going to be incremented. To minimize the drag force which is at this time, aircraft often use a slotted flap that might avoid separation.

One of the most applied techniques to support modern aerodynamics research is computational fluid dynamics. Computational fluid dynamics is the study of the use of computers for aiding in mathematical calculations or using mathematical models to perform the calculation over each divisor element, showing how to predict phenomena such as heat transfer, chemical reactions, and fluid flow patterns [2]. In view of the present scenario, the current analysis would focus on analysing the modification of a Cessna C 208b Grand Caravan due to a single slotted flap and effects produced by modifications in the coefficient of drag and coefficient of lift, comparison in values of CL/CD, Contour visualization of characteristics of vorticity, pressure, magnitude, and Velocity. Approaches to the study of fluid flow dynamics in slotted flaps were made by Kasem [3], Chapman [4], Fosteir [5], Velkovia [6, 7], and others. Todoirov [8] studied single-slotted flaps for lightweight wings. Numerical simulation will be performed using two-dimensional approach with the help of the Fluent software. The test object is a NACA 23012 airfoil with a flap deflection angle varying from 0° to 20° and a chord length of one meter. The fluid flow is configured with a Reynolds number (Re) = 3×10^6 under stable conditions. CFD simulations of the proposed wing with a single slotted flap demonstrated a higher lift coefficient compared to both the wing with a single plain flap and the baseline NACA 23012 airfoil. Additionally, the drag coefficient of the single slotted flap configuration was found to be lower than that of the single plain flap wing. Conversely, the single plain flap arrangement exhibited a higher drag coefficient.

This analysis also shows how the Wing Cessna C 208B Grand Caravan single slotted flap modification affects the value of the lift-to-drag ratio and C_L , C_D . Besides, the contour pressure coefficient, vorticity magnitude visualization and velocity of single-slotted flapping Cessna C208B Grand Caravan have been compared in the investigation.

2. METHOD

The three-dimensional numerical simulation will be employed in this strategy for searching. The program will be Ansys Fluent, and K-ɛ Realizable turbulent model will be used. Simulation consists of three stages that are: pre-processing, processing, and post-processing. According to Todorov's study, the test object employs a Cessna C208b Grand Caravan wing, the dimensions of which are 1:1 to the flap geometry and actual dimensions [8] in order to validate the results acquired.

2.1 boundary condition and simulation domain

A domain is a model that represents the test item. The domain determination has to be altered in order to have the results intended to be achieved, optimal conditions. [9]. In this case, the domain of the test section is a wing modeled as a wind tunnel. In Fig. 1, it is shown for each boundary condition. The aircraft's cruising speed or 96 (m/s) are the boundary conditions applied at the intake. Mulvany is a basis for compiling the simulation domain. [10] and Hayride's research [11] up to five chord lines behind the trailing edge (Fig. 2 and fig3).

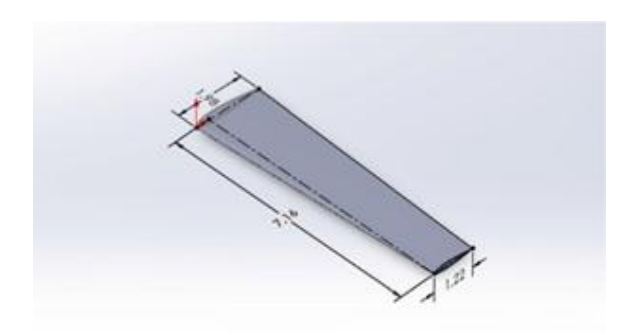


Figure 1. The simulation's wing geometry.

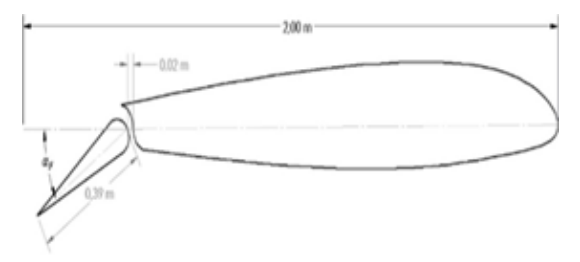
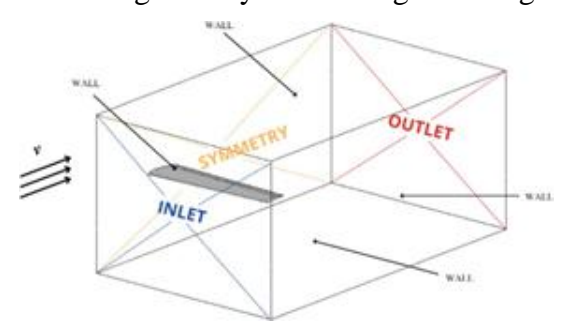


Figure 2. Simulation geometry of the wing with single slotted flap.



Configuration

Figure 3. Boundary condition and simulation domain.

2.1 Test of grid independence

Accurate data is required by the simulation software at both preprocessing and postprocessing stages. A grid independence test has to be done, which will tell the best grid structure and resolution that can approximate the actual conditions most accurately [12]. It ensures the repeatability of meshing and will define the best setting of a grid. The grid independence test compares different meshing types based on their numerical values of CD shown in Table 1. Each meshing type is tested for the least value of CD that can give a reliable and reasonably accurate result in the simulation. A low and consistent CD value is one of the factors taken into account in a numerical simulation. Thus, in accordance with Anderson's criterion, mesh five will serve as a reference for the next simulation. [13].

Table 1. Grid independence test results for test object without flap configuration.

Mesh Type	Element Count	Node Count	Drag Force (N)	Drag Coefficient (CD)
Mesh-1	2,973,528	536,344	551.932	0.007103
Mesh-2	3,144,327	567,622	551.113	0.007093
Mesh-3	3,342,603	603,273	552.029	0.007105
Mesh-4	3,579,492	646,215	554.961	0.007142
Mesh-5	3,985,830	719,004	552.925	0.007116

Mesh-6	4,345,541	783,368	553.072	0.007118
Mesh-7	4,776,373	861,801	554.978	0.007027
Mesh-8	5,308,558	957,603	554.463	0.007156
Mesh-9	5,830,581	1,049,415	551.257	0.007002
Mesh-10	6,472,375	1,090,534	552.242	0.007157

3. RESULT AND DISCUSSION

Numerical simulations of the Cessna 208b Grand Caravan wing were performed for various flap angles. Emphasis shall be placed on lift, drag, and the lift-to-drag ratio, supported by pressure coefficients, velocity contours, and vorticity magnitudes. Results provide insight into how changes in flap angle might affect aircraft performance across a variety of conditions.

3.1 velocity contour analysis

A line Velocity contours highlight flow behavior over the wing surface, revealing areas of acceleration, deceleration, and turbulence. At $\alpha F = 15^{\circ}$, a notable velocity differential develops between the upper and lower surfaces, enhancing lift production while introducing moderate turbulence near the trailing edge.

With $\alpha F = 30^{\circ}$, the airflow separates earlier along the upper surface, producing larger regions of recirculation and turbulence. At $\alpha = 16^{\circ}$, the separation zone expands significantly, leading to higher drag and reduced aerodynamic efficiency. This trend is consistent with pressure drops along the upper surface, causing increased adverse pressure gradients.

At lower RPM conditions (100, V = 3 m/s), displacement trends remain moderate, with minimal lift variations before stall. However, as RPM increases, the impact of lift augmentation becomes more pronounced. As shown in Figure 4, the displacement trends at RPM = 100 indicate a gradual increase in lift before stall, but with less intensity compared to higher RPM cases.

Simulations at $\alpha=0^\circ$ indicate minimal separation, with streamlined flow dominating. At $\alpha=8^\circ$, flow separation begins to emerge, growing substantially at $\alpha=16^\circ$. These observations underscore the importance of managing flap angles to balance lift and drag effectively across operational conditions.

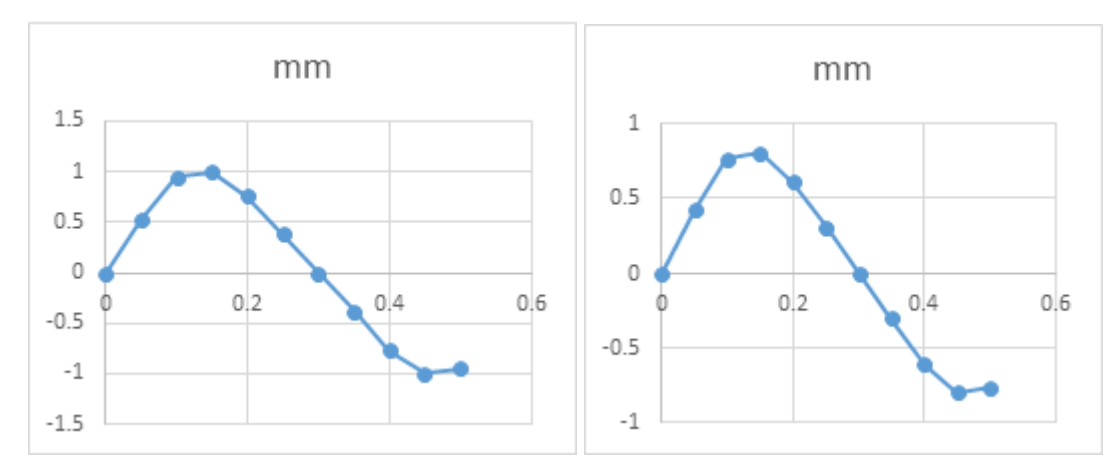


Figure. 4. Displacement vs. time at RPM = 100 and V = 3 m/s, illustrating baseline lift behavior before higher RPM effects are introduced.

3.2 pressure coefficient distribution

Pressure coefficient (Cp) contours reveal pressure variations across the wing. Higher flap angles amplify pressure changes, particularly near the leading edge, where low-pressure zones intensify.

At $\alpha F = 0^{\circ}$, pressure distribution remains smooth, minimizing flow separation. Increasing the flap angle to $\alpha F = 15^{\circ}$ generates stronger low-pressure zones along the upper surface, accelerating flow and increasing lift. At $\alpha F = 30^{\circ}$, Cp contours display broader low-pressure zones with irregular shapes, indicating turbulent flow and earlier separation.

The trailing edge shows higher pressures at larger flap angles, consistent with drag increases due to flow detachment and recirculation. These patterns align with lift and drag coefficients, affirming the impact of flap deflections on aerodynamic performance.

3.3 coefficient of lift

The The coefficient of lift (CL) was evaluated for flap angles (α F) of 0°, 15°, and 30° across various angles of attack (α). Figure 5 displays the relationship between CL and α .

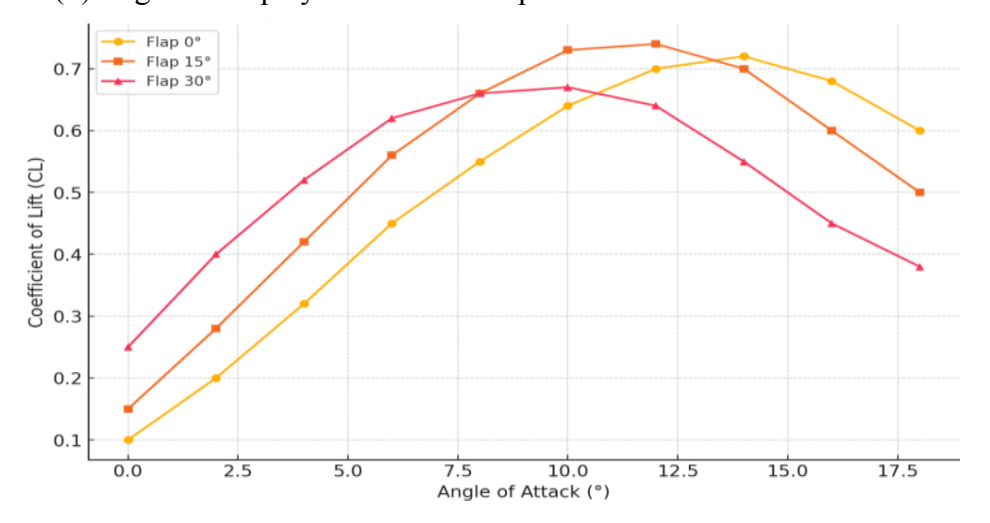


Figure 5. Coefficient of lift vs angle of attack.

Results reveal that increasing flap angles significantly enhances CL at lower angles of attack. For $\alpha F = 0^{\circ}$, the maximum CL achieved is approximately 0.745 at $\alpha = 18^{\circ}$. However, at $\alpha F = 30^{\circ}$, the maximum CL decreases slightly to 0.640 at $\alpha = 14^{\circ}$, indicating earlier stall due to increased flow separation. Despite this reduction in maximum CL, higher flap angles maintain improved lift performance at low attack angles, making them suitable for takeoff and landing phases.

At intermediate flap settings ($\alpha F = 15^{\circ}$), CL values are higher than at $\alpha F = 0^{\circ}$ but lower than at $\alpha F = 30^{\circ}$. This suggests that moderate flap angles balance lift enhancement and stall delay, offering flexibility in operational performance. Fig. 6 gives the variation of angular displacements w.r.t. angle of attack and CL for the following conditions: (a) RPM = 300, V = 10 m/s: Lift increases till stall conditions are reached. (b) RPM = 400, V = 14 m/s: The same effect is observed but more accentuated, demonstrating a stronger lift increase before stall.

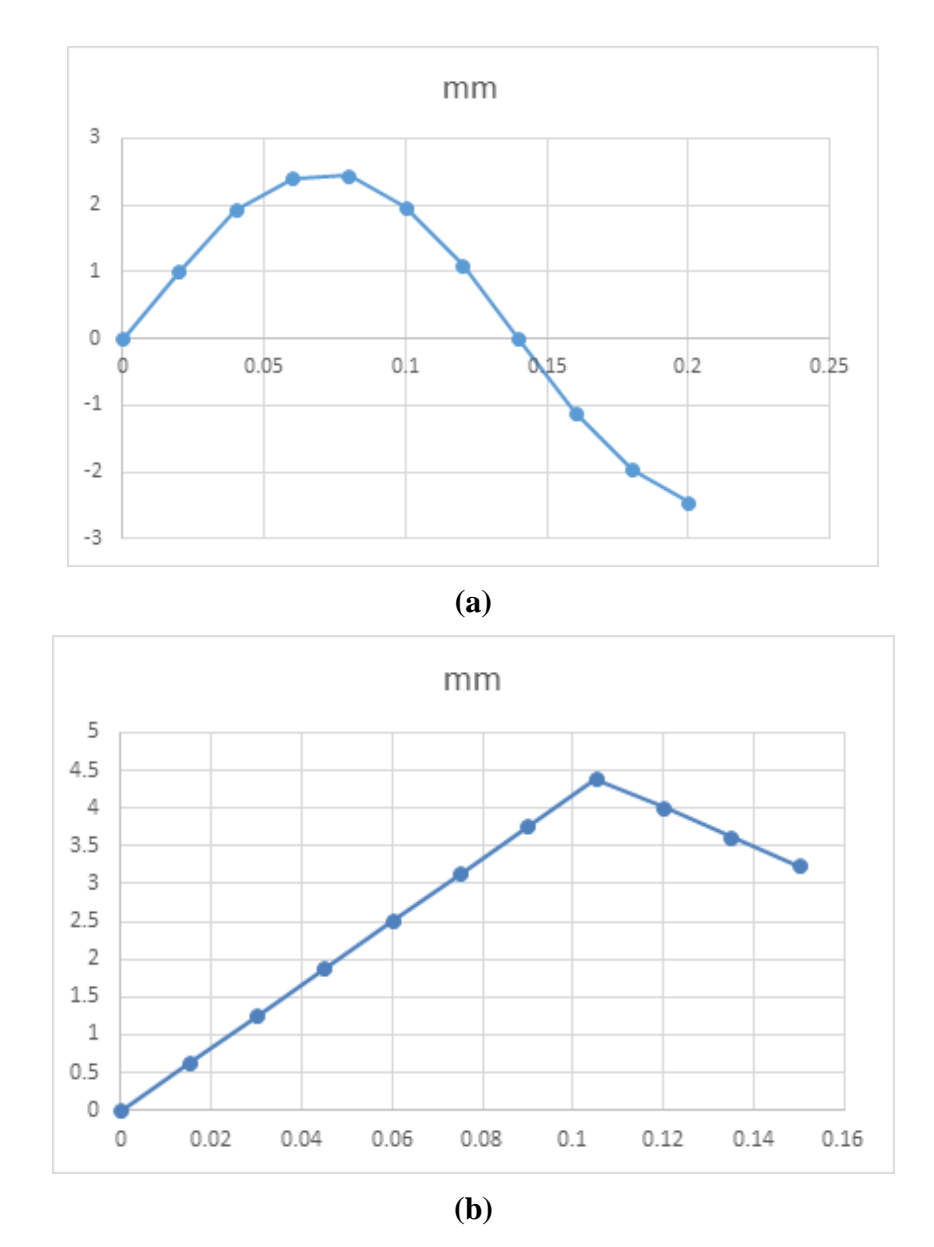


Figure 6. Displacement vs. time at varying RPMs: (a) RPM = 400, V = 14 m/s; (b) RPM = 300, V = 10 m/s, showing lift behavior leading up to stall.

3.4 coefficient of drag

Drag coefficient (CD) values corresponding to flap angles (α F) 0°, 15°, and 30° are shown in Figure 7. As expected, CD rises with increasing flap angles, due to larger exposed areas and enhanced flow disturbances.

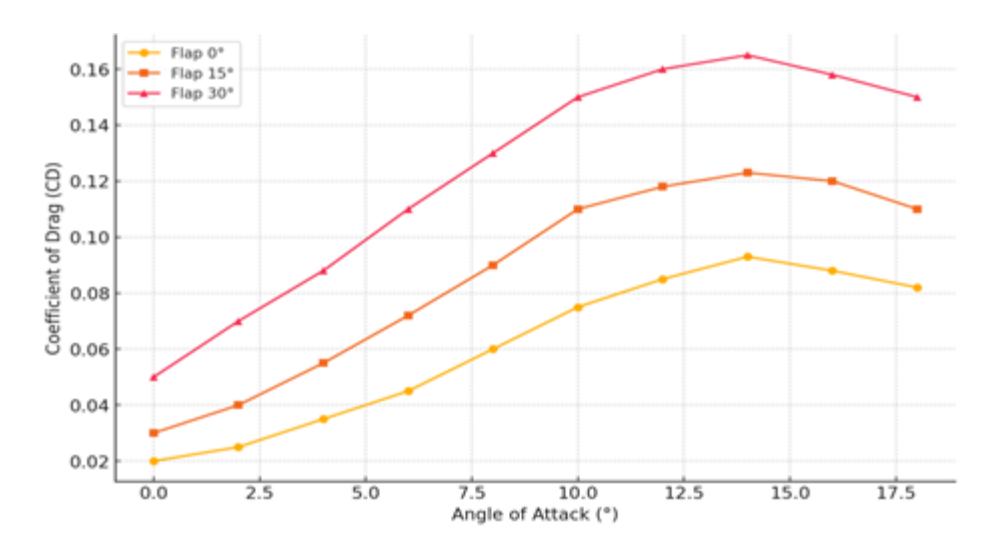


Figure 7. Coefficient of drag vs angle of attack.

For $\alpha F = 0^{\circ}$, drag remains relatively low, with a maximum value of 0.093 at $\alpha = 18^{\circ}$. At $\alpha F = 15^{\circ}$, the drag coefficient rises moderately to 0.123, while $\alpha F = 30^{\circ}$ produces the highest drag, peaking at 0.165. This behavior reflects the increased frontal area and stronger turbulence caused by larger flap deflections.

Higher drag at larger flap angles suggests a trade-off between lift enhancement and aerodynamic efficiency. While larger flap angles generate more lift, their higher drag coefficients emphasize their use during low-speed maneuvers, such as takeoff and landing, where enhanced lift compensates for drag penalties.

The coefficient of drag is directly affected by the displacement created because of aerodynamic resistance. From Figure 4, when RPM = 100 and V = 3 m/s, there is a progressive increase of the displacement against time due to the drag forces. For increased velocities, at RPM = 200 and V = 7 m/s in Figure 8, increased flow velocities produce an effect of the greatest oscillations of displacement amplitude.

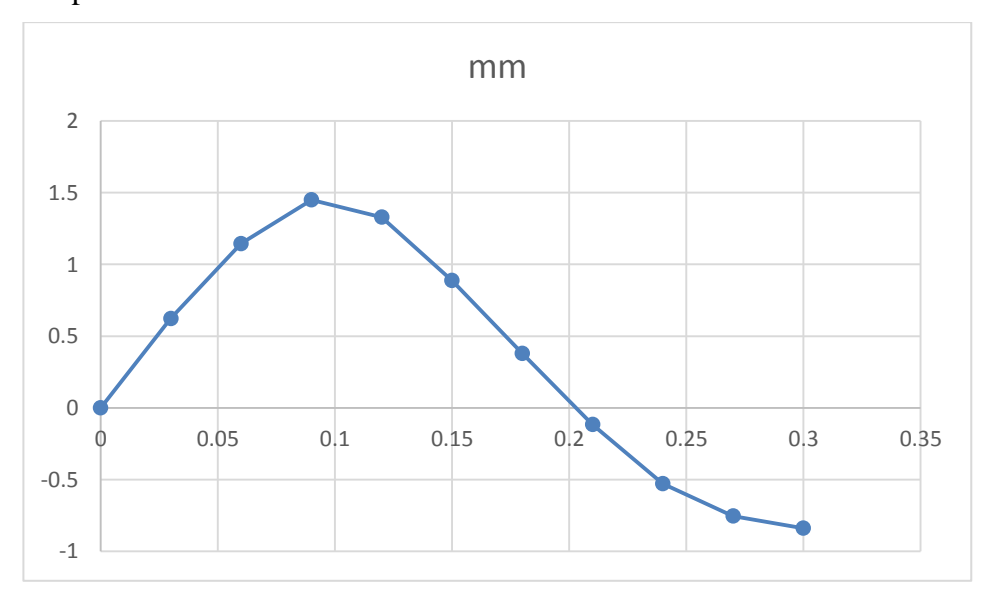


Figure. 8. Displacement vs. time at RPM = 200 and V = 7 m/s, demonstrating drag-induced oscillations in displacement over time.

3.5 lift-to-drag ratio

Figure 9 illustrates the variation of the lift-to-drag ratio (CL/CD) with angles of attack. The highest CL/CD value, approximately 13.80, is achieved at $\alpha = 8^{\circ}$ for $\alpha F = 0^{\circ}$. This configuration offers optimal aerodynamic efficiency, balancing lift and drag.

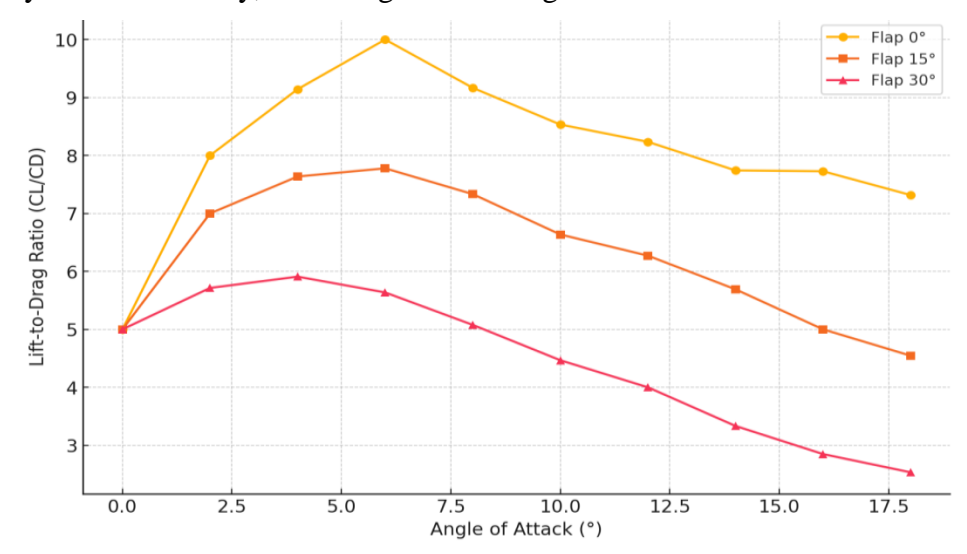


Figure 9. Lift-to-drag ratio vs angle of attack.

For $\alpha F = 15^{\circ}$, the peak CL/CD value drops slightly to 12.45, while $\alpha F = 30^{\circ}$ further reduces it to 10.20. Despite lower efficiency at higher flap angles, the enhanced lift production compensates for increased drag at lower speeds, providing better performance during takeoff and initial climb phases.

As the angle of attack increases, CL/CD values decrease across all flap angles due to drag buildup. These findings confirm that higher flap angles are more advantageous in scenarios prioritizing lift over efficiency.

The lift-to-drag ratio is the most important factor that determines the aerodynamic efficiency. Figure 10 shows how, for RPM = 400 and V = 14 m/s, the relationship between CL/CD varies with the change in flap deployment due to the changing trends of displacement.

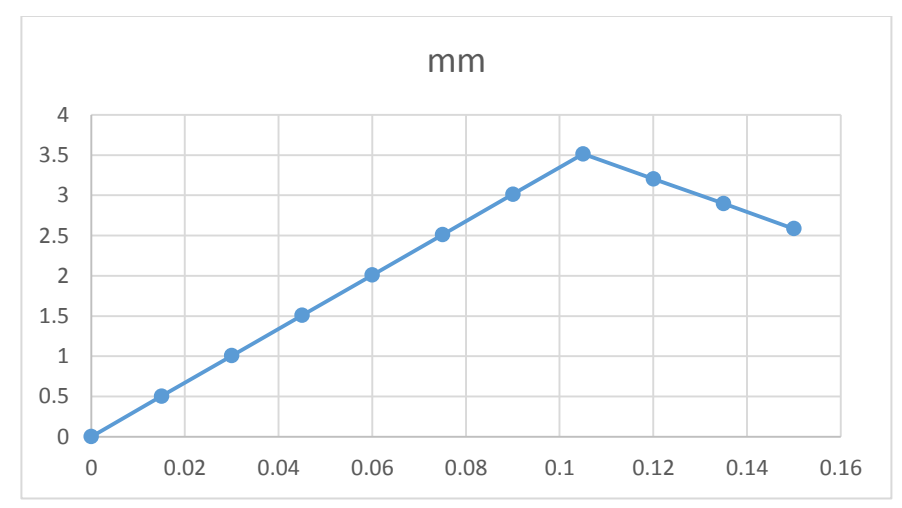


Figure 10. Displacement versus time at RPM = 400 and V = 14, representing the relationship between lift and drag efficiency.

3.6 vorticity magnitude contours

Figure 11 presents vorticity contours, illustrating flow rotation and turbulence. At $\alpha = 0^{\circ}$ and $\alpha F = 0^{\circ}$, vortices are compact and confined near the trailing edge. Increasing α to 8° elongates the vortex zones, reflecting stronger lift forces.

Higher flap angles produce more pronounced vortices, with $\alpha F = 30^{\circ}$ generating larger and more dispersed vortices. At $\alpha = 16^{\circ}$, turbulent regions intensify, emphasizing drag buildup and reduced aerodynamic efficiency.

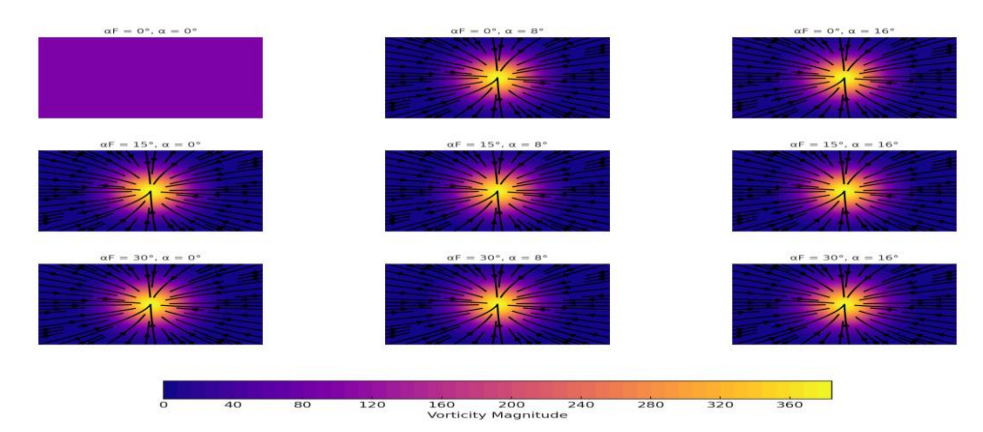


Figure 11. Vorticity magnitude contours - cessna 208b grand caravan.

4. CONCLUSION

The numerical simulation of the Cessna C208b Grand Caravan wing with single-slotted flap modifications provides the following conclusions:

- 1. Raising flap angles increases lift at low angles of attack, but reduces maximum CL values due to earlier stall.
- 2. Drag coefficients rise significantly with higher flap angles, emphasizing trade-offs between lift enhancement and aerodynamic efficiency.
- 3. Lift-to-drag ratios decrease with higher flap angles, yet maintain acceptable performance for takeoff and landing phases.
- 4. Velocity and pressure contours highlight intensified separation and turbulence at higher flap angles, aligning with observed lift and drag changes.
- 5. Vorticity analysis reveals stronger vortices at larger flap angles, confirming increased induced drag and flow disturbances.

These findings provide insights into optimizing wing configurations for different flight phases, balancing lift, drag, and aerodynamic efficiency through appropriate flap angle selections.

REFERENCES

- 1. J. Duncan, Pilot 's Handbook of Aeronautical Knowledge, Pilot. Handb. Aeronaut. Knowl.(2016) 524.
- 2. J.D. Anderson, Fundamentals of Aerodynamics (6th edition), McGraw-Hill, 2011.
- 3. K. Biber, Stall Hysteresis of an Airfoil with Slotted Flap, 42 (2005).
- 4. J. Chapman, Numerical Investigation of Flow Characteristics of a Slotted NACA 4414 Airfoil Numerical Investigation of Flow Characteristics of a Slotted NACA 4414 Airfoil, (2019).
- 5. D. Foster, H. Irwin, B. Williams, The Two-Dimensional Flow Around a Slotted Flap, Aeronaut. Res. Counc. Reports Memo. 3681. (1971).

- 6. C. Velkova, M. Todorov, Study of The Influence of A Gap between The Wing and SlottedFlap on The Aerodynamic Characteristics of Ultra-Light Aircraft Wing Airfoil, (2015).
- 7. C. Velkova, M. Todorov, G. Durand, Study the Influence of a Gap between the Wing and Slotted Flap over the Aerodynamic Characteristics of Ultra-Light Aircraft Wing Airfoil, 5 (2015) 278–285. https://doi.org/10.17265/2159-5275/2015.05.002.
- 8. M.D. Todorov, Aerodynamic Characteristics of Airfoil with Single Slotted Flap for LightAirplane Wing, (2015).
- 9. S.P. Setyo Hariyadi, Sutardi, W.A. Widodo, I. Sonhaji, Numerical Study of Secondary FlowCharacteristics on the Use of the Winglets, J. Phys. Conf. Ser. 1726 (2021). https://doi.org/10.1088/1742-6596/1726/1/012012.
- 10. N. Mulvany, L. Chen, J. Tu, B. Anderson, Steady-State Evaluation of Two-EquationRANS (Reynolds-Averaged Navier-Stokes) Turbulence Models for High-Reynolds Number Hydrodynamic Flow Simulations, Dep. Defence, Aust. Gov. (2004) 1–54.
- 11. S.P.S. Hariyadi, B. Junipitoyo, Sutardi, W.A. Widodo, Stall Behavior Curved Planform WingAnalysis with Low Reynolds Number on Aerodynamic Performances of Wing Airfoil Eppler 562, J. Mech. Eng. 19 (2022) 201–220.
- 12. S.P. Setyo Hariyadi, Sutardi, W.A. Widodo, M.A. Mustaghfirin, Aerodynamics Analysis of the Wingtip Fence Effect on UAV Wing, Int. Rev. Mech. Eng. 12 (2018). https://doi.org/10.15866/ireme.v12i10.15517.
- 13. J.D. Anderson, J.D. Anderson Jr, Computational Fluid Dynamics The Basics with Applications, 1995. https://doi.org/https://doi.org/10.1017/CBO9780511780066.
- 14. E.Q. Hussein, H.N. Azziz, F.L. Rashid, Aerodynamic Study of Slotted Flap for Naca 24012 Airfoil by Dynamic Mesh Techniques and Visualization Flow, J. Therm. Eng. 7 (2021) 230–239. https://doi.org/10.18186/THERMAL.871989.

Open Access This chapter is licensed under the terms of the Creative Commons AttributionNonCommercial 4.0 International License (http://creativecommons.org/licenses/by-nc/4.0/), which permits any noncommercial use, sharing, adaptation, distribution and reproduction in any medium or format, as long as you give appropriate credit to the original author(s) and the source, provide a link to the Creative Commons license and indicate if changes were made.

The images or other third party material in this chapter are included in the chapter's Creative Commons license, unless indicated otherwise in a credit line to the material. If material is not included in the chapter's Creative Commons license and your intended use is not permitted by statutory regulation or exceeds the permitted use, you will need to obtain permission directly from the copyright holder.